Langmuir

Article

pubs.acs.org/Langmuir

Solvent-Assisted Lipid Bilayer Formation on Silicon Dioxide and Gold

Seyed R. Tabaei,[†,‡] Jae-Hyeok Choi,[†,‡] Goh Haw Zan,[†,‡] Vladimir P. Zhdanov,[†,‡,∥] and Nam-Joon Cho*[,†,‡,§]

[†]School of Materials Science and Engineering, Nanyang Technological University, 50 Nanyang Avenue, 639798 Singapore

[‡]Centre for Biomimetic Sensor Science, Nanyang Technological University, 50 Nanyang Drive, 637553 Singapore

[§]School of Chemical and Biomedical Engineering, Nanyang Technological University, 60 Nanyang Drive, 637459 Singapore

[∥]Boreskov Institute of Catalysis, Russian Academy of Sciences, Novosibirsk 630090, Russia

Supporting Information

ABSTRACT: Planar lipid bilayers on solid supports mimic the fundamental structure of biological membranes and can be investigated using a wide range of surface-sensitive techniques. Despite these advantages, planar bilayer fabrication is challenging, and there are no simple universal methods to form such bilayers on diverse material substrates. One of the novel methods recently proposed and proven to form a planar bilayer on silicon dioxide involves lipid deposition in organic solvent and solvent exchange to influence the phase of adsorbed lipids. To scrutinize the specifics of this solvent-assisted lipid bilayer (SALB) formation method and clarify the limits of its applicability, we have developed a simplified, continuous solvent-exchange version to form planar bilayers on silicon dioxide, gold, and alkanethiol-coated gold (in the latter case, a lipid monolayer is formed to yield a hybrid bilayer) and varied the type of organic solvent and rate of solvent exchange. By tracking the SALB formation process with simultaneous quartz crystal microbalance−dissipation (QCM-D) and ellipsometry, it was determined that the acoustic, optical, and hydration masses along with the acoustic and optical thicknesses, measured at the end of the process, are comparable to those observed by employing conventional fabrication methods (e.g., vesicle fusion). As shown by QCM-D measurements, the obtained planar bilayers are highly resistant to protein adsorption, and several, but not all, water-miscible organic solvents could be successfully used in the SALB procedure, with isopropanol yielding particularly high-quality bilayers. In addition, fluorescence recovery after photobleaching (FRAP) measurements demonstrated that the coefficient of lateral lipid diffusion in the fabricated bilayers corresponds to that measured earlier in the planar bilayers formed by vesicle fusion. With increasing rate of solvent exchange, it was also observed that the bilayer became incomplete and a phenomenological model was developed in order to explain this feature. The results obtained allowed us to clarify and discriminate likely steps of the SALB formation process as well as determine the corresponding influence of organic solvent type and flow conditions on these steps. Taken together, the findings demonstrate that the SALB formation method can be adapted to a continuous solvent-exchange procedure that is technically minimal, quick, and efficient to form planar bilayers on solid supports.

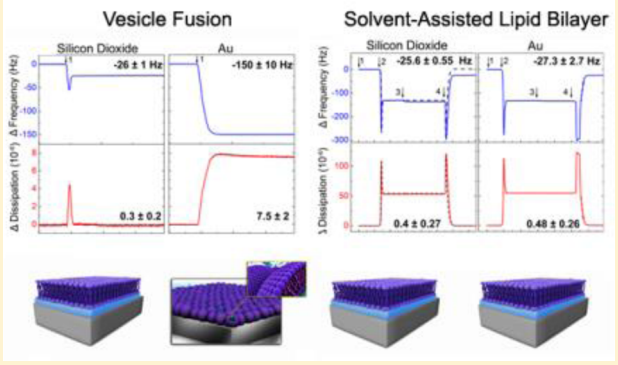

INTRODUCTION

A planar lipid bilayer formed on a solid support mimics the fundamental architecture of biological membranes and can be used to study various membrane processes.[1,2] There has been significant interest to develop a simple and robust technique for fabrication of such bilayers.[3] While many techniques can fabricate submicron-sized lipid spots and bilayer stacks, including air bubble collapse,[4] dip-pen nanolithography,[5] and spin-coating,[6] formation of a complete, planar bilayer is more challenging. At present, there are two widely adopted techniques to make planar bilayers that fully coat a solid support: Langmuir−Blodgett (LB) deposition[7] and more commonly vesicle fusion.[8] The latter involves vesicle adsorption and spontaneous rupture, which can occur via several mechanisms depending on the experimental conditions and vesicle characteristics.[9,10] Additional recently reported methods include those based on freezing and thawing,[11] detergents,[12] and peptide-induced vesicle rupture.[13] While these methods offer promising advantages, including possibly greater substrate range, vesicle fusion remains the most widely used method because it involves pure phospholipid vesicles and can promote bilayer self-assembly spontaneously at room temperature without the need for additional components.

A key feature of vesicle fusion is that planar bilayer formation typically occurs on a limited set of hydrophilic substrates such as borosilicate glass,[14,15] mica,[16,17] and silicon dioxide.[18] By

Received: December 21, 2013
Revised: July 19, 2014
Published: August 11, 2014

contrast, under physiological conditions, zwitterionic lipid vesicles adsorb and remain intact on gold,[19] titanium oxide,[20] and aluminum oxide[21] despite the observation of vesicle rupture in experiments employing more complex fabrication methods (see, e.g., ref 22 and references therein) and the fact that extended-DLVO calculations indicate that the lipid−substrate interaction on these surfaces may be more thermodynamically favorable, in some cases, than on bilayer-promoting substrates (e.g., silicon dioxide).[23] This limitation necessitates additional optimization of experimental conditions to promote vesicle rupture by various factors such as ionic strength,[24] solution pH,[25] osmotic shock,[26] and addition of divalent cations[27] or, as already mentioned, membrane-active peptides.[13] Vesicle properties can also be optimized/varied, including size,[28] lipid composition,[29] osmotic pressure,[30] and lamellarity.[31] Given the wide range of experimental parameters, it can be difficult to identify the right set of conditions to make a planar bilayer. Furthermore, vesicle fusion requires unilamellar vesicle preparation and quality control, both of which require moderate technical skill and resources. Considering the aforementioned issues, development of an alternative efficient method for bilayer formation would be highly advantageous.

Recently, Hohner et al.[32] demonstrated that incubation of phospholipids on silicon dioxide in an isopropanol/water mixture could result in formation of a planar bilayer upon a gradual increase in the solvent water fraction. In this method, inspired by reverse-phase evaporation used to form unilamellar vesicles in solution, gradual removal of the organic solvent (e.g., isopropanol) from the water−solvent mixture induces a series of phase transitions which lead to the formation of lamellar-phase structures.[32,33] Specifically, inverted micelles assembled in organic solution become unstable with increasing water content and are converted to monomers and then to conventional micelles and vesicles which helps to promote bilayer formation on the substrate.

One of the principal advantages of this approach is that different lipid assemblies (e.g., inverted micelles, monomers, or otherwise) can be directly used to form planar bilayers, bypassing the strict requirements for vesicle preparation. At the same time, the widespread utility of this method remains to be determined, including whether slow gradual titration of the solvent properties is required (as was used by Hohner et al.[32]) or a more rapid procedure can be implemented. Furthermore, it is important to determine if a solvent-assisted method based on this approach could be employed to form planar bilayers on substrates such as gold which is intractable to vesicle fusion. The quality of the bilayers formed should also be characterized. Bearing in mind all these aspects and using simultaneous quartz crystal microbalance-dissipation (QCM-D) and ellipsometry monitoring as well as fluorescence recovery after photobleaching (FRAP), we have investigated the process of solvent-assisted lipid bilayer (SALB) formation on silicon dioxide and gold and also explored the influence of organic solvent type and solvent-exchange rate to form high-quality planar lipid bilayers. Lipid monolayer formation on alkanethiol-covered gold was also tested. Our results presented below show that the SALB formation method allows one to fabricate a good-quality planar lipid bilayer in about 30 min, hence demonstrating that the method is efficient and potentially amenable to wide application.

MATERIALS AND METHODS

Lipid Preparation. Zwitterionic lipid, 1,2-dioleoyl-*sn*-glycero-3-phosphocholine (DOPC), and fluorescently labeled lipid, 1,2-dioleoyl-*sn*-glycero-3-phosphoethanolamine-*N*-(lissamine rhodamine B sulfonyl) (ammonium salt), were purchased from Avanti Polar Lipids (Alabaster, AL). For SALB experiments, lipid powder was dissolved immediately before experiment in the appropriate organic solvent at 10 mg/mL lipid concentration and then diluted accordingly to the desired final lipid concentration. Extruded vesicles employed for vesicle fusion experiments were prepared using 50 nm diameter pore, track-etched polycarbonate membranes, and 10 mM Tris buffer (pH 7.5) with 150 mM NaCl, as previously described.[34]

Quartz Crystal Microbalance−Dissipation (QCM-D). A Q-Sense E4 instrument (Q-Sense AB, Gothenburg, Sweden) was used to monitor the lipid deposition process in real time. Changes in the resonance frequency and energy dissipation of a 5 MHz AT-cut piezoelectric quartz crystal were recorded at the 3rd, 5th, 7th, 9th, and 11th overtones. The QCM-D silicon dioxide-coated substrates (Q-Sense AB) are composed of quartz crystals coated with the following layers and corresponding thicknesses in sequential order: 10 nm Cr, 100 nm Au, 10 nm Ti, and last 50 nm SiO_2. Layers were coated by using the physical vapor deposition (PVD) method. The root-mean-square (RMS) roughness was 1.2 ± 0.1 nm according to the manufacturer. The QCM-D gold-coated substrates (Q-Sense AB) are composed of quartz crystals coated with the following layers and corresponding thicknesses in sequential order: 10 nm Cr and then 100 nm Au. The layers were also coated by using the PVD method. The surface roughness was 0.9 ± 0.2 nm according to the manufacturer. Thiolated gold crystals were prepared by incubation overnight with 1 mM 1-octadecanethiol in ethanol. All measurements were done under flow-through conditions at a flow rate of 50 μL/min (unless otherwise noted), by using a Reglo Digital peristaltic pump (Ismatec, Glattbrugg, Switzerland). The experimental temperature was fixed at 24.0 ± 0.5 °C. All surfaces were treated with oxygen plasma at 180 W for 1 min (March Plasmod Plasma Etcher, March Instruments, Concord, CA) immediately before use.

QCM-D experimental data collected at the 3rd, 5th, 7th, and 9th overtones were analyzed by using the Voigt−Voinova model, as previously reported.[35−38] The Voigt−Voinova model is strictly valid for homogeneous thin films (e.g., planar lipid bilayers), and the parameters obtained from the model representation may be interpreted as effective parameters rather than absolute parameters for adsorbed vesicle layers (see, e.g., ref 38 for further discussion on this subject). In the model, for such cases, the vesicle adlayer was treated as a homogeneous adlayer (lipid vesicles and hydrodynamically coupled solvent inside and between vesicles) with a uniform density of 1000 kg m^{-3}, and the viscosity of the bulk aqueous solution was constrained to be 0.001 Pa s^{-1} in order to determine an effective film thickness (in turn, yielding the effective Voigt mass) and effective film viscosity. From such model estimations, previous attempts have been made to compare acoustically and optically measured masses (the latter being measured by reflectometry[39,40] or ellipsometry,[41] for example) of vesicle adlayers, and we follow a similar treatment here using ellipsometry.

Combined Quartz Crystal Microbalance−Dissipation (QCM-D) and Ellipsometry. Simultaneous QCM-D and ellipsometry measurements were performed by using a Q-Sense E1 module (Q-Sense AB, Gothenburg, Sweden) and a Nanofilm EP3 ellipsometer (Accurion GmbH, Germany). Ellipsometric measurements were controlled with the EP3View software (Accurion GmbH). The Nanofilm EP3 ellipsometer employs a PCSA configuration in order to determine the rotation angles of the polarizer and analyzer that lead to nulling conditions for retrieving the parameters, Δ and Ψ, which quantify the change in the light polarization through the ratio of the reflection coefficient of p- and s-polarized light, $r_p/r_s = \tan \Psi e^{i\Delta}$. Incident light with a wavelength of 545.6 nm was selected from a xenon lamp by using an interference filter. The measured Δ and Ψ were fit to a layered structure in order to obtain the complex refractive index and thickness of each layer by using the EP4 model software

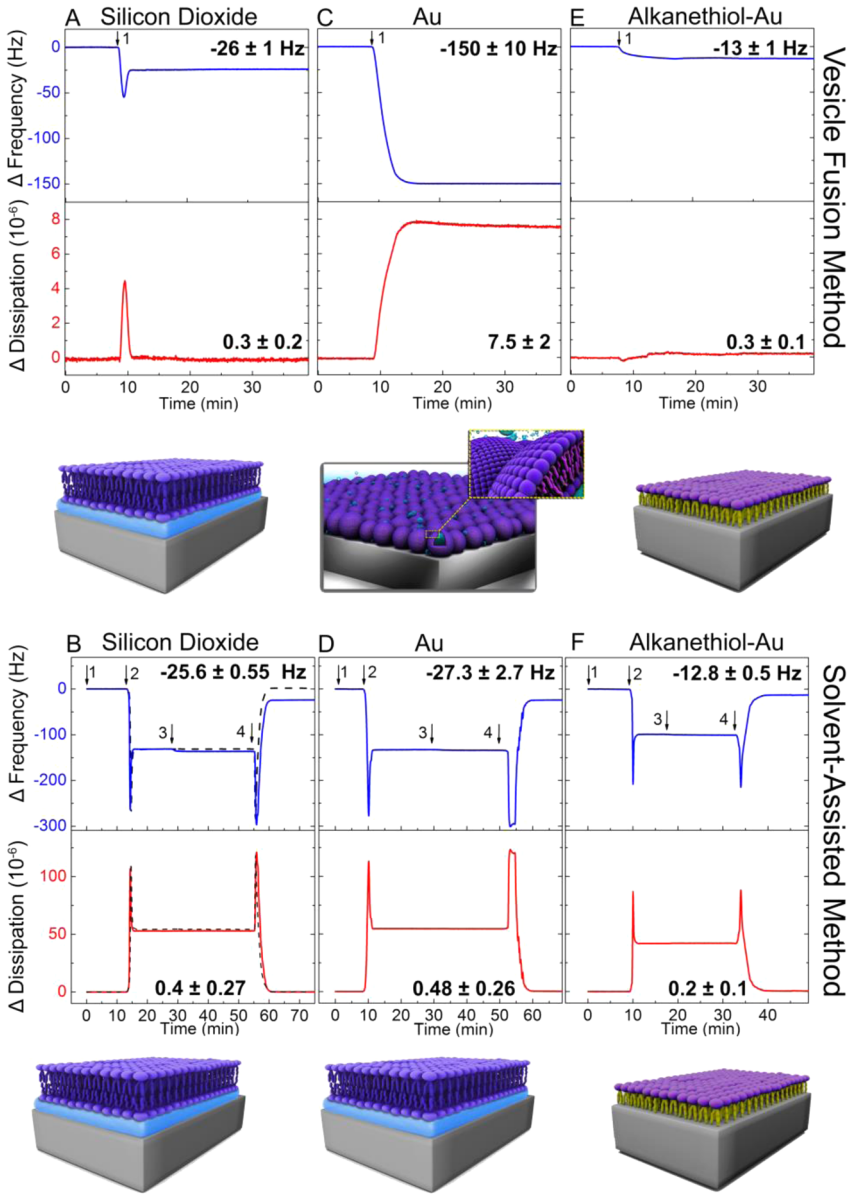

Figure 1. QCM-D monitoring of vesicle fusion and SALB methods on three different substrates. QCM-D frequency shift (Δf, blue) and dissipation shift (ΔD, red) for the third overtone (n = 3) were measured as a function of time during lipid adsorption onto (A, B) silicon dioxide, (C, D) gold, and (E, F) alkanethiol-coated gold. Panels, A, C, and E correspond to the vesicle fusion method. DOPC lipid vesicles were added at t = 10 min (arrow 1) after establishing the baseline for the frequency and dissipation shifts. Panels B, D, and F correspond to the SALB formation method. Arrows indicate the injection of buffer [10 mM Tris, 150 mM NaCl, pH 7.5; (1)], isopropanol (2), lipid mixture [0.5 mg/mL DOPC lipid in isopropanol; (3)], and buffer exchange (4). The dashed curve in panel B represents the control experiment in which lipid was not injected (see Figure S1 for magnified view). The final values of Δf and ΔD for each surface are reported. All values are given as the mean of at least three runs. The schematics show the proposed assembled lipid structures as inferred from the final frequency and dissipation shifts.

(Accurion GmbH). To obtain the optical and structural properties of the substrates, measurements were carried out in air or buffer (n_{buffer} = 1.336). For gold surfaces, with a nominal thickness of ~100 nm which renders the surfaces opaque, the gold was treated as a semi-infinite thick layer, and its refractive index n and the extinction coefficient k were obtained directly from the measurements under buffer. For silicon dioxide surfaces, measurements in air and buffer were required for obtaining the optical properties of the substrate, which was a layer of silicon dioxide on top of opaque titanium. Additionally, the lipids deposited on these substrates were modeled as a homogeneous layer with a refractive index n_{layer} and a thickness d_{layer}.[42] n_{layer} was constrained from 1.336 (refractive index of buffer) to 1.5 (refractive index of a lipid bilayer), and d_{layer} was constrained from 0 to 100 nm. Subsequently, the optical mass of this layer, $\Delta m_{optical}$, was obtained from n_{layer} and d_{layer} by using the de Feijter formula.[43] To use this formula, the dn/dc value of lipids must be known to high accuracy. For lipids, the dn/dc value is reported from 0.11 to 0.18 mL/g in the literature.[44−50] Furthermore, ellipsometry is particularly sensitive to optical anisotropy which arises when lipids are in the absorbed state[44,51] because the technique measures the relative change in reflection for s- and p-polarized light, and it is not known if the dn/dc value of lipid vesicles in solution is equal to the dn/dc value of a planar bilayer on different solid supports. Therefore, in this case, we use dn/dc = 0.16 mL/g on silicon dioxide and 0.12 mL/g on gold to ensure the optical mass of the final bilayers is in the neighborhood of 400 ng/

dx.doi.org/10.1021/la501534f | Langmuir 2014, 30, 10363−10373

cm^2,[40] which is the expected areal mass density and is consistent with the acoustic mass recorded by the QCM-D measurements.

Matrix-Assisted Laser Desorption Ionization Time-of-Flight (MALDI-TOF) Mass Spectrometry. Experiments were carried out using a Shimadzu Biotech Axima TOF mass spectrometer equipped with a pulsed nitrogen laser (337 nm wavelength with <3.5 ns pulses). Data acquisition was performed in the reflector positive ion mode to scan from 50 to 2000 (m/z) with a sensitivity to distinguish 1 part per 6000. Each mass spectrum was an average of 50 profiles with 20 shots per profile. Prior to MALDI experiments, the samples were covered with the MALDI matrix (20 mg/mL solution of 2,5-dihydroxybenzoic acid (DHB) in Milli-Q-treated water) and air-dried again.

Fluorescence Microscopy and Fluorescence Recovery after Photobleaching (FRAP). Fluorescence microscopy imaging of supported planar bilayers containing 0.5 wt % rhodamine-modified phospholipid was performed by using an inverted epifluorescence Eclipse TE 2000 microscope (Nikon) equipped with a 60× oil immersion objective (NA 1.49) and an Andor iXon+ EMCCD camera (Andor Technology, Belfast, Northern Ireland). The acquired images consisted of 512 × 512 pixels with a pixel size of 0.267 × 0.267 μm. The samples were illuminated through a TRITC (rhodamine−DHPE) filter set by a mercury lamp (Intensilight C-HGFIE; Nikon Corporation). For FRAP measurements, a 30 μm wide circular spot was photobleached with a 532 nm, 100 mW laser beam, followed by time-lapsed recording. Diffusion coefficients were determined by the Hankel transform method,[52] along with immobile fraction. For all fluorescence imaging experiments, glass coverslips (Menzel Gläser, Braunschweig, Germany) were used. For FRAP experiments involving the SALB procedure, commercially available microfluidic flow cells (stick-Slide I0.1 Luer, Ibidi, Munich, Germany) were employed, with an injection flow rate of 50 μL/min.

RESULTS AND DISCUSSION

The phase behavior of phospholipids in isopropanol/water mixtures has previously been quantified in detail.[32] With increasing water mole fraction, lipids can self-assemble into various states from inverse micelles at low water content to monomers, micelles, and vesicles at moderate and high water contents. If lipids are near a glass surface, then a gradual increase in the solvent's water content (stepwise from 0 to ∼90%) can induce them to form a planar bilayer as was demonstrated on silicon dioxide.[32] We hypothesized that a gradual solvent-exchange procedure involving buffer addition to deposited lipids in organic solvent could be a quicker route to form bilayers on hydrophilic substrates in general, including those which are intractable to vesicle fusion. To test this hypothesis, we employed QCM-D tracking in order to monitor the time-resolved kinetics of lipid adsorption onto solid supports. This technique measures changes in the resonance frequency (Δf) and energy dissipation (ΔD) related to an adsorbate's mass and viscoelastic properties, respectively.[53] For comparison, lipid deposition by two methods, SALB and vesicle fusion, was performed on silicon dioxide, gold, and alkanethiol-coated gold (Figure 1).

For vesicle fusion experiments, a baseline was first established in aqueous buffer solution (Figures 1A,C,E). Then, vesicles in an identical buffer solution were added at t = 10 min. For SALB experiments, aqueous buffer solution was the initial condition for QCM-D measurements in order to establish baseline signals (Figures 1B,D,F, arrow 1). After 15 min stabilization, isopropanol was injected (Figures 1B,D,F, arrow 2), and the changes in density and viscosity led to large changes in resonance frequency and energy dissipation, including a short transient period during mixing. After an additional 15 min stabilization, 0.5 mg/mL DOPC lipid in isopropanol was injected (Figures 1B,D,F, arrow 3), which led to a small change in resonance frequency and no change in the energy dissipation. Finally, the solution was gradually replaced with aqueous buffer solution, equivalent to that used in the baseline measurement (Figures 1B,D,F, arrow 4).

SALB on Silicon Dioxide. For vesicle fusion on silicon dioxide, characteristic two-step adsorption kinetics was observed (Figure 1A). The first step involved vesicle adsorption until reaching a critical coverage, as denoted by maximum changes in the QCM-D measurement signals (Δf and ΔD shifts of −60 Hz and 4 × 10^{-6}, respectively). The critical coverage denotes the point at which the combination of vesicle−substrate and vesicle−vesicle interactions becomes sufficient to cause vesicle rupture accompanied by the release of coupled solvent from vesicles. In turn, there is a decrease in adsorbed mass and the final changes are consistent with a planar bilayer[54] (Δf and ΔD shifts of −26 ± 1 Hz and (0.3 ± 0.2) × 10^{-6}, respectively).

In the corresponding SALB experiments with QCM-D monitoring (Figure 1B), once the SALB procedure was finished as described above, the Δf and ΔD values were consistent with previous QCM-D responses for planar lipid bilayer formation[54] (Δf and ΔD shifts of −25.6 ± 0.55 Hz and (0.4 ± 0.27) × 10^{-6}, respectively). Interestingly, lipid deposition in organic solvent was observed (Δf and ΔD shifts of −5.2 Hz and 0.1 × 10^{-6}, respectively; Figure 1B and Figure S1). A control experiment (black, dotted curve in Figure 1B) was performed using an identical procedure, albeit without lipid. In this case, there was no change in measurement signal at step 3, further supporting that lipid adsorption in organic solvent occurs. Moreover, the final measurement values in the control experiment were equivalent to the baseline. This confirms that no other mass was adsorbed onto the substrate and that the final changes in measurement values associated with bilayer formation upon stabilization at each step are due to lipid adsorption. Overall, the findings support that, on silicon dioxide, planar lipid bilayers can be formed by using both methods.

As organic solvent (isopropanol) was used in the SALB procedure, we also attempted to check if there was any isopropanol remaining after formation of the planar bilayer. Although in general the direct detection of residual solvent in a planar bilayer is difficult, preliminary MALDI-TOF mass spectrometry measurements indicate that the amount of residual solvent in the bilayer was, at most, low (see Figure S3). To quantify the amount of residual solvent, if present, further studies would be required, and we have instead focused on characterizing the structural properties of the bilayers formed via the SALB method in comparison to bilayers (or other lipid structures) fabricated via the vesicle fusion method. From this viewpoint, we next explored if the SALB method could form planar bilayers on a substrate which is intractable to the vesicle fusion method.

SALB on Gold. Planar bilayer formation on gold has been difficult to achieve by using vesicle fusion. In this case, vesicles typically adsorb and do not rupture.[54] As demonstrated in Figure 1C, vesicle addition onto the gold surface led to the formation of an adsorbed layer of intact vesicles (Δf and ΔD shifts of −150 ± 10 Hz and (7.5 ± 2) × 10^{-6}, respectively). Although there are several reports on formation of "hybrid bilayer membranes" on thiolipid-modified gold surfaces,[55,56] there is only one method available to form planar bilayers on gold, which is to add a specific amphipathic, α-helical (AH) peptide that is known to induce vesicle rupture.[13] Based on the aforementioned experimental results on silicon dioxide, the

SALB method, if successful, would have several potential advantages to form bilayers on gold. It does not require vesicles and the bilayer properties appear to be identical independent of whether vesicle fusion or SALB was employed.

We therefore performed a SALB experiment on gold. Strikingly, in contrast to the results obtained earlier with vesicle fusion, we observed here planar bilayer formation with Δf and ΔD shifts of -27.3 ± 2.7 Hz and $(0.48 \pm 0.26) \times 10^{-6}$, respectively (Figure 1D). We also observed lipid adsorption in isopropanol prior to bilayer formation. A key observation was that the kinetics of lipid deposition using SALB on gold was qualitatively similar to that of silicon dioxide (Figure 1B), suggesting that the formation mechanism differs from what conventionally works for bilayer formation on solid supports via vesicle fusion. In practice, as already noted, it is possible to convert the adsorbed, intact vesicle layer into a bilayer by employing an amphipathic peptide[13] in order to induce vesicle rupture, but it takes extra steps and an additional component is needed. Our present work shows that these shortcomings can be bypassed by using the SALB formation method.

Taking into account that (i) vesicle rupture is typically a limiting step in the vesicle fusion method and (ii) this step does not occur on gold, while (iii) the SALB formation method works in this case, we can conclude that vesicle formation and subsequent rupture do not seem to play a role in the SALB formation process.

Compared to existing bilayer fabrication strategies on gold,[13] the SALB method is much simpler and takes advantage of how lipids self-assemble in different solvents.

SALB on Alkanethiol-Coated Gold. In the case of vesicle adsorption on alkanethiol-coated gold, a lipid monolayer (Δf shift of -12.8 ± 0.5 Hz) was formed with one-step kinetics (Figure 1E) as earlier was reported.[54] In contrast to the silicon dioxide case, vesicles rupture immediately upon adsorption onto the methyl-terminated monolayer, and thus there is no frequency minimum prior to rupture. In both cases, the energy dissipations were smaller than $(0.3 \pm 0.1) \times 10^{-6}$, signaling the rigidity of the formed structures. Figure 1F displays the QCM-D results of the SALB experiment applied to the hydrophobic alkanethiol surface. Experimentally, the same four stages as in case of silicon dioxide were repeated. The final frequency value after complete solvent-exchange was 12.8 ± 0.5 Hz, i.e., half of that typically observed for bilayer formation, suggesting deposition of a lipid monolayer. On the basis of the experiments above, the SALB procedure appears to make it possible to form planar bilayers on hydrophilic solid supports and monolayers on hydrophobic solid supports.

Simultaneous QCM-D and Ellipsometry Measurements. To further characterize the adsorbed lipid layers on silicon dioxide and gold produced by the vesicle fusion and SALB methods, ellipsometry was used simultaneously. The corresponding measurements were conducted in parallel with QCM-D monitoring utilizing a combined QCM-D and ellipsometry setup. QCM-D measurements determine the hydrated mass, including mass of the adsorbed lipid film and mass of the solvent that is coupled to the film. The solvent mass is referred to as the hydration mass. In the planar lipid bilayer system, a major contribution to the hydration mass is related to the thin hydration layer which separates the lipid bilayer from the substrate. On the other hand, ellipsometry measures the thickness of the adsorbed film, excluding the associated solvent molecules.[57] Therefore, ellipsometry can be used to calculate the dry mass of the film.[58] Hence, the mass properties of lipid bilayers formed could be compared across different substrates and formation methods.

The acoustic, optical, and hydration masses (the latter being the difference between the acoustic and optical masses) as well as the corresponding effective thicknesses of the adsorbed layers are presented in Figures 2A,B (see Figure S2 for QCM-D and ellipsometry measurement data). For the case of silicon dioxide, the lipid bilayers formed by both vesicle fusion and SALB procedures were similar and had acoustic and optical masses around 450 and 400 ng/cm^2, respectively. In each case, the corresponding hydration mass was therefore approximately 50 ng/cm^2. For the layers on silicon dioxide, the acoustic thicknesses obtained via the vesicle fusion and SALB methods were also nearly similar (4.6 ± 0.1 and 4.5 nm, respectively). Likewise, the corresponding optical thicknesses were 5.1 ± 2.5 and 3.7 nm, respectively, which are in the range expected for a planar bilayer (roughly between 3.5 and 5.5 nm; see, e.g., ref 44).

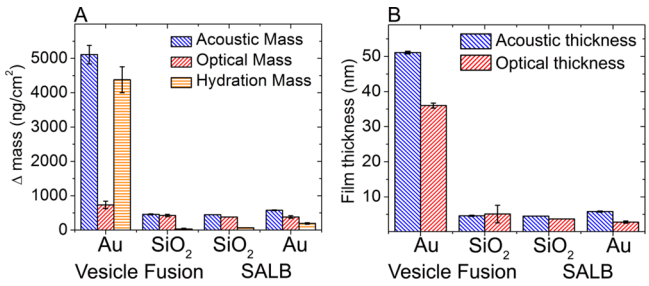

Figure 2. Mass and thickness of adsorbed lipid films produced by vesicle fusion and SALB methods on silicon dioxide and gold. Summary of (A) optical, acoustic, and hydration masses and (B) thickness of lipid layers from two different formation methods: vesicle fusion and SALB. Bilayer formation was monitored by simultaneous QCM-D and ellipsometry measurement. Acoustic and optical film thicknesses of the obtained lipid layer on each surface were calculated based on the final values of the QCM-D and ellipsometry measurements. QCM-D and ellipsometry data were analyzed using the Voigt–Voinova model and de Feijter equation, respectively.

For lipid layers on gold, the difference between the vesicle fusion and SALB formation methods was more distinct. Using vesicle fusion, an adsorbed vesicle layer formed and the acoustic and optical thicknesses were approximately 5100 and 700 ng/cm^2, respectively. The difference indicates that coupled solvent contributed significantly to the total adsorbed mass which is expected for a layer of intact vesicles. Furthermore, the acoustic and optical thicknesses of the layer were 51.1 ± 0.3 and 36 ± 0.7 nm, respectively. By contrast, for SALB-formed lipid layers on gold, the mass and thickness of the film were significantly smaller. In this case, the acoustic and optical masses were approximately 570 and 380 ng/cm^2, respectively. The corresponding hydration mass was about 190 ng/cm^2, which is appreciably larger than the hydration mass determined for bilayers on silicon dioxide that were formed by either the vesicle fusion or SALB method. This difference in the hydration mass may be related to a greater hydration force for lipid–substrate interactions on gold, and recent findings[59] suggest that, among interfacial forces described in extended-DLVO models, the hydration force has a particularly strong contribution to influence vesicle adhesion on titanium oxide, including attachment and rupture. A relatively high hydration force in this case would help explain why vesicles do not

dx.doi.org/10.1021/la501534f | Langmuir 2014, 30, 10363–10373

rupture on gold in analogy with titanium oxide—both of which have appreciably greater Hamaker constants than silicon dioxide.[60,61]

In addition, the acoustic and optical thicknesses obtained for the SALB-formed bilayer on gold were 5.8 ± 0.1 and 2.8 ± 0.3 nm, respectively, the former of which is consistent with the expected range for a hydrated planar bilayer.[62] In this case, the relatively small optical thickness is outside the expected range and suggests that the optical properties of the bilayer on gold (and its corresponding thick hydration layer) may differ from those of silica-supported bilayers, for which more structural information is currently available. By employing alternative formation methods such as the SALB procedure, more detailed structural information about planar bilayers on gold may become available by using informative techniques such as neutron reflectometry[63] in due course. In the present case, the simultaneous QCM-D and ellipsometry measurements verify that planar lipid bilayers formed on silicon dioxide via either the vesicle fusion or SALB procedure have comparable mass properties (acoustic, optical, and hydration) and that the planar bilayer formed on gold via the SALB procedure has a comparable optical mass but greater acoustic mass and accordingly higher hydration mass. Taken together, the results support that the SALB procedure allows one to form planar bilayers which have comparable global properties to bilayers formed on the same substrates via the vesicle fusion method.

Protein Adsorption on Planar Lipid Bilayers. To further scrutinize the homogeneity of SALB-formed bilayers, we studied adsorption of proteins at planar bilayers fabricated on silicon dioxide and gold. While QCM-D and ellipsometry measurements involving lipid adsorption assume the lipid layers to be homogeneous films and provide quantitative information about global adlayer properties (e.g., mass and thickness), protein adsorption experiments allow one to characterize an adlayer locally, including the presence of defects. Planar bilayers of zwitterionic lipid composition are highly resistant to adsorption of proteins such as, e.g., bovine serum albumin (BSA; this globular protein is relatively stable in the adsorbed state).[64] By contrast, nonspecific protein adsorption on hydrophilic oxide films is generally appreciable.[65] Hence, in principle, protein adsorption on a defect-free bilayer would be negligible, and an increasing amount of bound protein suggests the presence of defects, e.g., availability of hydrophilic substrate sites for protein attachment.

With QCM-D monitoring, we quantified BSA adsorption onto the bilayer-coated and bare substrates (Figure S4). On bare silicon dioxide, BSA adsorption led to a frequency shift of −17 Hz. By contrast, BSA adsorption at an SALB-formed bilayer on silicon dioxide resulted in a frequency shift of only −1 ± 0.5 Hz, a reduction of greater than 94%. Similar results were obtained on gold. The frequency shifts corresponding to BSA adsorption at a bare gold substrate and at an SALB-formed bilayer on gold were −27 and −2 ± 0.8 Hz, respectively. In this case, the reduction in protein adsorption was greater than 92%. From these experiments in combination with the QCM-D and ellipsometry measurements, we conclude that SALB-formed bilayers on silicon dioxide and gold are homogeneous and fully coat the surface. As with planar bilayers formed by vesicle fusion, a small level of defects is inevitably present,[66] and BSA protein adsorption as described here could also be useful as a blocking step to prevent further nonspecific adsorption on either the substrate or bilayer.

Effect of Solvent-Exchange Rate on SALB Formation Process. To further understand the specifics of the SALB formation process, we also investigated the influence of solvent-exchange rate. For these experiments, the SALB procedure was performed on silicon dioxide by using two different lipid concentrations (0.125 and 0.5 mg/mL). For each set of experiments, the exchange step from lipids in organic solvent to aqueous buffer in the SALB procedure was performed at two different flow velocities (2.05×10^{-4} and 1.23×10^{-3} m/s, respectively). Figure 3 demonstrates QCM-D measurement

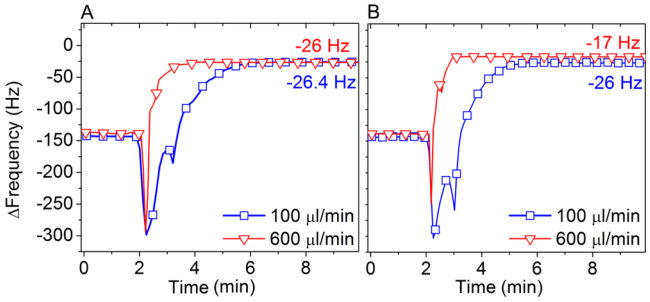

Figure 3. Influence of the solvent-exchange rate on the SALB formation process. QCM-D frequency shifts (Δf) corresponding to the final step (see Arrow 4 in Figure 1B) in the SALB method were measured on silicon dioxide at two different exchange rates, 100 and 600 μL/min, using (A) 0.5 and (B) 0.125 mg/mL DOPC lipid in isopropanol. The final Δf values are also specified, as compared to the measurement baseline in aqueous buffer solution.

responses upon replacement of lipid/isopropanol by aqueous buffer. In the case of 0.5 mg/mL DOPC lipid (Figure 3A), the flow rate did not affect the bilayer formation, and at both flow rates a final frequency of approximately −26 Hz was obtained. By contrast, at 0.125 mg/mL DOPC lipid (Figure 3B), the amount of adsorbed lipid at the final step was significantly affected by flow rate. At an average flow rate of 100 μL/min (corresponding to a flow velocity of 2.05×10^{-4} m/s), bilayer formation was complete, and a final frequency of −26 Hz was obtained. However, at a 6-fold higher flow rate (600 μL/min corresponding to a flow velocity of 1.23×10^{-3} m/s), a final frequency of −17 Hz was obtained, which corresponds to an incomplete bilayer.

In analogy with the DMPC lipids,[32] DOPC lipids in organic solution are expected to consist of nonlamellar phases (e.g., monomers and inverted micelles). In this solution, under steady-state conditions, planar lipid bilayer formation is thermodynamically unfavorable, and lipid uptake by the surface is comparatively low (see Figure 1 and Figure S1) and insufficient to form a complete planar bilayer. With increasing water content, as already noted in the Introduction, inverted micelles become unstable and are eventually converted to conventional micelles and eventually, at high water content, may be converted to vesicles.[32] Under the transient conditions in our measurements, the formation of the lipid bilayer on the surface may occur via several channels including adsorption and decomposition of inverted and/or conventional micelles, decomposition of micelles in the solution and adsorption of the decomposition products (e.g., monomers), decomposition of micelles followed by formation of vesicles, and their adsorption and rupture. Monomers can, however, be excluded because in the coexistence region their concentration is low. Vesicles can, in fact, be excluded as well as already was argued in the aforementioned gold case (in addition, this pathway

dx.doi.org/10.1021/la501534f | Langmuir 2014, 30, 10363−10373

appears to be unlikely because it includes too many steps). Thus, adsorption and rupture of inverted or conventional micelles seem to play a key role in planar bilayer formation. Focusing on these two channels, we discuss below the role of the solvent-exchange rate in the SALB formation process. To be specific, we imply that it occurs primarily with participation of conventional micelles because adsorption of inverted micelles in organic solution is largely negligible with regards to the lipid supply necessary to form a complete planar bilayer.

Interpretation of the experiments under consideration is complicated by slow diffusion of micelles. Because of this factor, their spatial distribution during the solvent exchange may be complex, especially under transient flow conditions. To avoid these complications, we use a coarse-grained model and operate with average lipid mass concentration, c, in the solution and use the effective rate constants of micelle attachment to the support, k_a, and micelle decomposition not resulting in attachment, k_d. To validate this approach, we note that the QCM-D sensor surface is relatively large and basically the QCM-D-measured kinetics are sensitive to the average concentrations. Concerning micelle attachment, our remark is that the corresponding rate constant may in reality depend on time. This dependence is, however, minor compared to that related to solvent exchange, and we neglect it.

In our analysis, the initial time, $t = 0$, is identified with the beginning of the replacement of the organic solution by aqueous buffer. If the water concentration is low, conventional micelles are either absent or stable and do not adsorb. This initial phase is described as

$$dc/dt = -\gamma c \quad \text{or} \quad c = c_0 \exp(-\gamma t) \tag{1}$$

where c_0 is the initial lipid concentration and $\gamma = F/V$ is the solvent exchange constant (F is the average flow rate and V is the cell volume). Note that eq 1 is valid irrespective of whether lipids are in the phase of inverted micelles, monomers, or conventional micelles.

The fraction of organic solvent in the cell is described in analogy:

$$C = C_0 \exp(-\gamma t) \tag{2}$$

As soon as C decreases down to the critical value, C_*, and accordingly the water concentration become appreciable, lipid is in the phase of conventional micelles, and these micelles can attach to the surface and form a lipid bilayer and decompose in solution. At this stage, taking place at

$$t \geq t_* \equiv \ln(C_0/C_*)/\gamma \tag{3}$$

Equation 1 can be extended as

$$dc/dt = -(k_a + k_d + \gamma)c \tag{4}$$

This equation implies that lipids are in the phase of conventional micelles.

To integrate eq 4, we consider that the loss of lipid in the solution is related primarily with the solvent exchange or decomposition. This is reasonable because the contribution of lipids forming the planar lipid bilayer relative to the global lipid balance is minor. Under such conditions, we drop k_a in the right-hand part of eq 4 and obtain

$$c = c_0 \exp[-\gamma t_* - (k_d + \gamma)(t - t_*)] \tag{5}$$

The amount of adsorbed micelles is then given by

$$U = k_a \int_{t_*}^{\infty} c(t)\, dt = \frac{k_a}{k_d + \gamma} c_0 \exp(-\gamma t_*) \tag{6}$$

Taking into account that t_* is defined by (3), we rewrite (6) as

$$U = C_* k_a c_0 / [C_0(k_d + \gamma)] \tag{7}$$

Assuming the decomposition of adsorbed micelles to be rapid, we identify U with a lipid bilayer. Expression 7 is applicable provided $U \leq U_b$, where U_b is the amount of adsorbed micelles needed to form a planar lipid bilayer. With this condition, expression 7 shows that (i) the bilayer formation is complete and does not depend on γ if c_0 is sufficiently high so that $U \gg U_b$, (ii) the bilayer formation does not depend on γ also provided $k_d \gg \gamma$, and (iii) if, on the other hand, k_d is comparable to or lower than γ and c_0 is not sufficiently large, then the formation of the lipid bilayer may become incomplete with increasing γ. Predictions i and iii are in agreement with the experiment. These findings clarify at least to some extent the likely mechanistic details behind our observations and also the basic requirements for successful bilayer formation via the SALB procedure in isopropanol solution. With the proven effectiveness of isopropanol as a solvent in this case, we next investigated whether the SALB procedure could be performed with other organic solvents as well.

Effects of Organic Solvent on SALB Procedure. In addition to isopropanol, four more organic solvents were selected for testing, including ethanol, *n*-propanol, methanol, and acetonitrile. The principal selection criterion was 100% water miscibility. In three out of the four cases, the SALB formation process executed as described above was successful. The only exception was the acetonitrile case, hence demonstrating that the SALB procedure is not applicable to all water-miscible organic solvents. Furthermore, the QCM-D measurement responses reflecting the global properties of the bilayers formed varied depending on the solvent employed (Figures 4A,B). The final Δf values for isopropanol, ethanol,

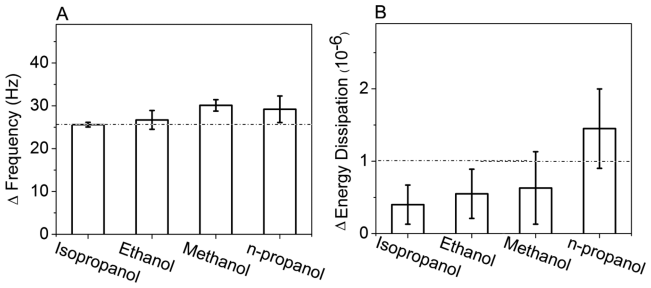

Figure 4. Effect of organic solvent type on lipid layers formed via the SALB method. Summary of final (A) frequency shifts (Δf) and (B) dissipation shifts (ΔD) obtained from QCM-D experiments for 0.5 mg/mL DOPC lipid adsorption on silicon dioxide by using different organic solvents. The dotted lines correspond to $\Delta f = -26$ Hz and $\Delta D = 1 \times 10^{-6}$.

methanol, and *n*-propanol were 25.6 ± 0.55, 26.7 ± 2.2, 30.1 ± 1.34, and 29.2 ± 3.1 Hz, respectively, and the corresponding ΔD values were 0.4 ± 0.27, 0.55 ± 0.34, 0.63 ± 0.5, and 1.45 ± 0.55 $\times 10^{-6}$, respecttively. It has been established that planar bilayer formation leads to changes in frequency of approximately −26 Hz and energy dissipation of less than 0.5×10^{-6}. Therefore, on the basis of these criteria, we evaluated the quality of the formed bilayers. The deviation of the acquired Δf and ΔD shifts from the aforementioned values is due to the

dx.doi.org/10.1021/la501534f | Langmuir 2014, 30, 10363−10373

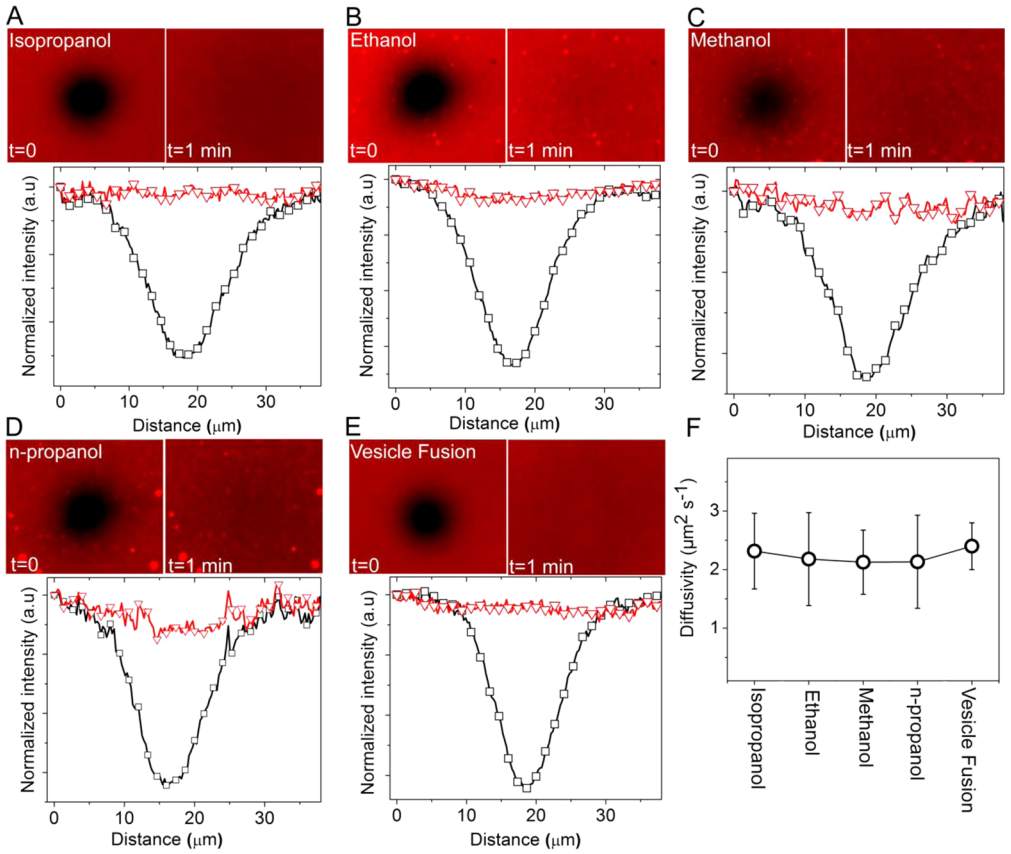

Figure 5. FRAP snapshots of bilayers prepared by the SALB method using different organic solvents. Fluorescence microscopy images (100 × 100 μm) of DOPC lipid bilayers containing 0.5 wt % Rho-PE lipid formed on glass surfaces via the SALB method using lipid solutions in (A) isopropanol, (B) ethanol, (C) methanol, or (D) *n*-propanol and (E) bilayer formed by vesicle fusion. The bright spots in panels B–D correspond to lipid aggregates. Right and left images were taken immediately and after 1 min photobleaching, respectively. The normalized intensity profiles of the bleached spots before (black squares) and after recovery (red triangles) are presented. (F) Summary of corresponding diffusion coefficients of lipid bilayers prepared via the SALB and vesicle fusion methods, the former of which was performed using different organic solvents. The measurements were repeated three times, and each FRAP measurement was repeated at least 10 times per sample.

presence of additional mass which exceeds that required to form a complete bilayer and contributes some viscoelastic element. For instance, the dissipation values obtained in the methanol and *n*-propanol cases are higher than what is expected for a defect-free homogeneous bilayer. In particular, in the case of *n*-propanol, both the final Δf and ΔD values diverge from those of a single bilayer. By contrast, isopropanol shows low energy dissipation and a frequency shift of 26.6 ± 0.55 Hz, which indicates formation of a continuous single bilayer.

In order to further analyze the physical properties of planar bilayers formed via the SALB method with different organic solvents, the homogeneity and fluidity of bilayers were characterized by fluorescence microscopy and fluorescence recovery after photobleaching (FRAP), respectively (Figure 5). Figures 5A–D show images of the corresponding bilayers prepared by using different solvents, immediately after photobleaching (left) and after 1 min recovery (right). The FRAP snapshots of the bilayer fabricated by vesicle fusion are shown in Figure 5E. The homogeneous fluorescence microscopy images of the SALB bilayer fabricated by isopropanol (Figure 5A) and the bilayer prepared by vesicle fusion (Figure 5E) suggest the formation of globally uniform and defect-free bilayers. The intensity profiles show that the fluorescence recovery was almost complete in 1 min for all samples, indicating that the lipids are laterally mobile. The FRAP data were analyzed by using the Hankel transform method, yielding an average diffusion coefficient of 2.2 ± 0.1 $\mu m^2/s$ in all cases (Figure 5F), which is in good agreement with the range of diffusivity expected for a fluid planar bilayer.[7,67,68]

All bilayers except the one prepared by *n*-propanol generally had 96% or greater mobile fractions. The bilayer formed via *n*-propanol had a lower mobile fraction (90%). Evaluation of bilayer quality based on the homogeneity of the fluorescence microscopy images and FRAP results is consistent with the QCM-D results. As depicted in the fluorescence microscopy images (Figures 5C,D), the bilayers formed by using methanol (Figure 5C) and *n*-propanol (Figure 5D) are not homogeneous. Such inhomogeneity is caused by lipid aggregates that coexist with the lipid bilayer. Such defects are likely responsible for the higher immobile fraction observed in the bilayer formed using *n*-propanol. These observations are consistent with the QCM-D results obtained for the cases of methanol and *n*-propanol (Figures 4A,B). In both cases, the Δf and ΔD shifts deviate from the expected values for a planar bilayer. On the basis of the QCM-D measurement data and the fluorescence microscopy analysis, the findings support that, among the tested solvents and conditions, isopropanol appears particularly well-suited to form good-quality bilayers via the SALB procedure. Overall, the type of organic solvent used appears to be an important parameter to optimize SALB formation.

dx.doi.org/10.1021/la501534f | *Langmuir* 2014, 30, 10363–10373

CONCLUSION

Herein, we have comprehensively scrutinized from different perspectives the use of the SALB method to form planar lipid bilayers on solid supports, including silicon dioxide and gold. In particular, the roles of solvent type and flow conditions have been shown. The quality of the fabricated bilayer has been characterized in detail. In addition, a lipid monolayer on alkanethiol-covered gold was also formed in a similar way. Finally, we repeat that the SALB method does not require vesicle preparation, which permits bilayer formation in a simpler, more versatile, and quicker way that is independent of surface properties within the tested range. Although further studies are needed in order to more deeply elucidate the corresponding mechanism of bilayer formation, our findings suggest that the SALB method may serve as a general and efficient tool to form planar bilayers on solid supports.

ASSOCIATED CONTENT

Supporting Information

More detailed information about lipid adsorption in isopropanol solution (Figure S1), experimental data from simultaneous QCM-D and ellipsometry measurements (Figure S2), MALDI-TOF mass spectrometry experimental data for SALB-formed planar bilayer characterization (Figure S3), and protein adsorption experimental data from QCM-D measurements (Figure S4). This material is available free of charge via the Internet at http://pubs.acs.org.

AUTHOR INFORMATION

Corresponding Author

*E-mail: njcho@ntu.edu.sg (N.-J.C.).

Notes

The authors declare no competing financial interest.

ACKNOWLEDGMENTS

The authors acknowledge support from the National Research Foundation (NRF-NRFF2011-01), the National Medical Research Council (NMRC/CBRG/0005/2012), and Nanyang Technological University to N.J.C. V.P.Zh. is a recipient of the Tan Chin Tuan Exchange Fellowship at Nanyang Technological University.

REFERENCES

(1) Sackmann, E. Supported membranes: Scientific and practical applications. *Science* **1996**, *271* (5245), 43−48.
(2) Johnson, S. J.; Bayerl, T. M.; McDermott, D. C.; Adam, G. W.; Rennie, A. R.; Thomas, R. K.; Sackmann, E. Structure of an adsorbed dimyristoylphosphatidylcholine bilayer measured with specular reflection of neutrons. *Biophys. J.* **1991**, *59* (2), 289−294.
(3) Edward, T.; Castellana; Cremer, P. S. Solid supported lipid bilayers: From biophysical studies to sensor design. *Surf. Sci. Rep.* **2006**, *61*, 429−444.
(4) Mager, M. D.; Melosh, N. A. Lipid bilayer deposition and patterning via air bubble collapse. *Langmuir* **2007**, *23* (18), 9369−9377.
(5) Lenhert, S.; Sun, P.; Wang, Y.; Fuchs, H.; Mirkin, C. A. Massively parallel dip-pen nanolithography of heterogeneous supported phospholipid multilayer patterns. *Small* **2007**, *3* (1), 71−75.
(6) Mennicke, U.; Salditt, T. Preparation of solid-supported lipid bilayers by spin-coating. *Langmuir* **2002**, *18* (21), 8172−8177.
(7) Tamm, L. K.; McConnell, H. M. Supported phospholipid bilayers. *Biophys. J.* **1985**, *47* (1), 105−113.
(8) Kalb, E.; Frey, S.; Tamm, L. K. Formation of supported planar bilayers by fusion of vesicles to supported phospholipid monolayers. *Biochim. Biophys. Acta* **1992**, *1103* (2), 307−16.
(9) Richter, R.; Mukhopadhyay, A.; Brisson, A. Pathways of lipid vesicle deposition on solid surfaces: a combined QCM-D and AFM study. *Biophys. J.* **2003**, *85* (5), 3035−3047.
(10) Reimhult, E.; Zäch, M.; Höök, F.; Kasemo, B. A multitechnique study of liposome adsorption on Au and lipid bilayer formation on SiO_2. *Langmuir* **2006**, *22* (7), 3313−3319.
(11) Sugihara, K.; Jang, B.; Schneider, M.; Voros, J.; Zambelli, T. A universal method for planar lipid bilayer formation by freeze and thaw. *Soft Matter* **2012**, *8* (20), 5525−5531.
(12) Vacklin, H. P.; Tiberg, F.; Thomas, R. K. Formation of supported phospholipid bilayers, via co-adsorption with beta-D-dodecyl maltoside. *Biochim. Biophys. Acta, Biomembr.* **2005**, *1668* (1), 17−24.
(13) Cho, N. J.; Cho, S. J.; Cheong, K. H.; Glenn, J. S.; Frank, C. W. Employing an amphipathic viral peptide to create a lipid bilayer on Au and TiO_2. *J. Am. Chem. Soc.* **2007**, *129* (33), 10050−10051.
(14) Weirich, K. L.; Israelachvili, J. N.; Fygenson, D. K. Bilayer edges catalyze supported lipid bilayer formation. *Biophys. J.* **2010**, *98* (1), 85−92.
(15) Cremer, P. S.; Boxer, S. G. Formation and spreading of lipid bilayers on planar glass supports. *J. Phys. Chem. B* **1999**, *103* (13), 2554−2559.
(16) Zasadzinski, J. A. N.; Helm, C. A.; Longo, M. L.; Weisenhorn, A. L.; Gould, S. A. C.; Hansma, P. K. Atomic force microscopy of hydrated phosphatidylethanolamine bilayers. *Biophys. J.* **1991**, *59* (3), 755−760.
(17) Egawa, H.; Furusawa, K. Liposome adhesion on mica surface studied by atomic force microscopy. *Langmuir* **1999**, *15* (5), 1660−1666.
(18) Seeger, H. M.; Cerbo, A. D.; Alessandrini, A.; Facci, P. Supported lipid bilayers on mica and silicon oxide: comparison of the main phase transition behavior. *J. Phys. Chem. B* **2010**, *114* (27), 8926−8933.
(19) Keller, C.; Glasmästar, K.; Zhdanov, V.; Kasemo, B. Formation of supported membranes from vesicles. *Phys. Rev. Lett.* **2000**, *84* (23), 5443.
(20) Reviakine, I.; Rossetti, F. F.; Morozov, A. N.; Textor, M. Investigating the properties of supported vesicular layers on titanium dioxide by quartz crystal microbalance with dissipation measurements. *J. Chem. Phys.* **2005**, *122*, 204711.
(21) Mager, M. D.; Almquist, B.; Melosh, N. A. Formation and characterization of fluid lipid bilayers on alumina. *Langmuir* **2008**, *24* (22), 12734−12737.
(22) Hardy, G. J.; Nayak, R.; Zauscher, S. Model cell membranes: Techniques to form complex biomimetic supported lipid bilayers via vesicle fusion. *Curr. Opin. Colloid Interface Sci.* **2013**, *18* (5), 448−458.
(23) Tero, R.; Ujihara, T.; Urisu, T. Lipid bilayer membrane with atomic step structure: supported bilayer on a step-and-terrace TiO2 (100) surface. *Langmuir* **2008**, *24* (20), 11567−11576.
(24) Boudard, S.; Seantier, B.; Breffa, C.; Decher, G.; Felix, O. Controlling the pathway of formation of supported lipid bilayers of DMPC by varying the sodium chloride concentration. *Thin Solid Films* **2006**, *495* (1-2), 246−251.
(25) Cho, N.-J.; Jackman, J. A.; Liu, M.; Frank, C. W. pH-Driven assembly of various supported lipid platforms: A comparative study on silicon oxide and titanium oxide. *Langmuir* **2011**, *27* (7), 3739−3748.
(26) Stanglmaier, S.; Hertrich, S.; Fritz, K.; Moulin, J. F.; Haese-Seiller, M.; Rädler, J. O.; Nickel, B. Asymmetric distribution of anionic phospholipids in supported lipid bilayers. *Langmuir* **2012**, *28* (29), 10818−10821.
(27) Rossetti, F. F.; Bally, M.; Michel, R.; Textor, M.; Reviakine, I. Interactions between titanium dioxide and phosphatidyl serine-containing liposomes: formation and patterning of supported phospholipid bilayers on the surface of a medically relevant material. *Langmuir* **2005**, *21* (14), 6443−6450.

(28) Reimhult, E.; Höök, F.; Kasemo, B. Vesicle adsorption on SiO_2 and TiO_2: Dependence on vesicle size. *J. Chem. Phys.* **2002**, *117* (16), 7401−7404.
(29) Hamai, C.; Yang, T.; Kataoka, S.; Cremer, P. S.; Musser, S. M. Effect of average phospholipid curvature on supported bilayer formation on glass by vesicle fusion. *Biophys. J. 90* (4), 1241−1248.
(30) Jackman, J. A.; Choi, J.-H.; Zhdanov, V. P.; Cho, N.-J. Influence of osmotic pressure on adhesion of lipid vesicles to solid supports. *Langmuir* **2013**, *29* (36), 11375−11384.
(31) Jackman, J. A.; Zhao, Z.; Zhdanov, V. P.; Frank, C. W.; Cho, N.-J. Vesicle adhesion and rupture on silicon oxide: Influence of freeze−thaw pretreatment. *Langmuir* **2014**, *30* (8), 2152−2160.
(32) Hohner, A.; David, M.; Rädlera, J. Controlled solvent-exchange deposition of phospholipid membranes onto solid surfaces. *Biointerphases* **2010**, *5* (1), 1−8.
(33) Szoka, F.; Papahadjopoulos, D. Procedure for preparation of liposomes with large internal aqueous space and high capture by reverse-phase evaporation. *Proc. Natl. Acad. Sci. U. S. A.* **1978**, *75* (9), 4194−4198.
(34) MacDonald, R. C.; MacDonald, R. I.; Menco, B. P. M.; Takeshita, K.; Subbarao, N. K.; Hu, L. R. Small-volume extrusion apparatus for preparation of large, unilamellar vesicles. *Biochim. Biophys. Acta, Biomembr.* **1991**, *1061* (2), 297−303.
(35) Reviakine, I.; Rossetti, F. F.; Morozov, A. N.; Textor, M. Investigating the properties of supported vesicular layers on titanium dioxide by quartz crystal microbalance with dissipation measurements. *J. Chem. Phys.* **2005**, *122* (20), 204711.
(36) Cho, N.-J.; Kanazawa, K. K.; Glenn, J. S.; Frank, C. W. Employing two different quartz crystal microbalance models to study changes in viscoelastic behavior upon transformation of lipid vesicles to a bilayer on a gold surface. *Anal. Chem.* **2007**, *79* (18), 7027−7035.
(37) Patel, A. R.; Frank, C. W. Quantitative analysis of tethered vesicle assemblies by quartz crystal microbalance with dissipation monitoring: binding dynamics and bound water content. *Langmuir* **2006**, *22* (18), 7587−7599.
(38) Ohlsson, G.; Tigerström, A.; Höök, F.; Kasemo, B. Phase transitions in adsorbed lipid vesicles measured using a quartz crystal microbalance with dissipation monitoring. *Soft Matter* **2011**, *7* (22), 10749−10755.
(39) Edvardsson, M.; Svedhem, S.; Wang, G.; Richter, R.; Rodahl, M.; Kasemo, B. QCM-D and reflectometry instrument: applications to supported lipid structures and their biomolecular interactions. *Anal. Chem.* **2008**, *81* (1), 349−361.
(40) Cho, N. J.; Wang, G. L.; Edvardsson, M.; Glenn, J. S.; Höök, F.; Frank, C. W. Alpha-helical peptide-induced vesicle rupture revealing new insight into the vesicle fusion process as monitored in situ by quartz crystal microbalance-dissipation and reflectometry. *Anal. Chem.* **2009**, *81* (12), 4752−4761.
(41) Goh, H. Z.; Cho, N.-J. Rupture of zwitterionic lipid vesicles by an amphipathic, α-helical peptide: indirect effects of sensor surface and implications for experimental analysis. *Colloids Surf., B* **2014**, in press.
(42) Benes, M.; Billy, D.; Benda, A.; Speijer, H.; Hof, M.; Hermens, W. T. Surface-dependent transitions during self-assembly of phospholipid membranes on mica, silica, and glass. *Langmuir* **2004**, *20* (23), 10129−10137.
(43) De Feijter, J. A.; Benjamins, J.; Veer, F. A. Ellipsometry as a tool to study the adsorption behavior of synthetic and biopolymers at the air-water interface. *Biopolymers* **1978**, *17*, 1759−72.
(44) Mashaghi, A.; Swann, M.; Popplewell, J.; Textor, M.; Reimhult, E. Optical anisotropy of supported lipid structures probed by waveguide spectroscopy and its application to study of supported lipid bilayer formation kinetics. *Anal. Chem.* **2008**, *80* (10), 3666−3676.
(45) Merz, C.; Knoll, W.; Textor, M.; Reimhult, E. Formation of supported bacterial lipid membrane mimics. *Biointerphases* **2008**, *3* (2), Fa41−Fa50.
(46) Erbe, A.; Sigel, R. Tilt angle of lipid acyl chains in unilamellar vesicles determined by ellipsometric light scattering. *Eur. Phys. J. E* **2007**, *22* (4), 303−309.
(47) Chong, C. S.; Colbow, K. Light-scattering and turbidity measurements on lipid vesicles. *Biochim. Biophys. Acta* **1976**, *436* (2), 260−282.
(48) Brandrup, J.; Immergut, E. H.; Grulke, E. A. *Polymer Handbook*, 4th ed.; Wiley: New York, 1999.
(49) Riske, K. A.; Politi, M. J.; F. Reed, W.; Lamy-Freund, M. T. Temperature and ionic strength dependent light scattering of DMPG dispersions. *Chem. Phys. Lipids* **1997**, *89* (1), 31−44.
(50) Yi, P. N.; Macdonal, R. C. Temperature-dependence of optical properties of aqueous dispersions of phosphatidylcholine. *Chem. Phys. Lipids* **1973**, *11* (2), 114−134.
(51) Salamon, Z.; Tollin, G. Optical anisotropy in lipid bilayer membranes: Coupled plasmon-waveguide resonance measurements of molecular orientation, polarizability, and shape. *Biophys. J.* **2001**, *80* (3), 1557−1567.
(52) Jonsson, P.; Jonsson, M. P.; Tegenfeldt, J. O.; Höök, F. A method improving the accuracy of fluorescence recovery after photobleaching analysis. *Biophys. J.* **2008**, *95* (11), 5334−5348.
(53) Rodahl, M.; Höök, F.; Krozer, A.; Brzezinski, P.; Kasemo, B. Quartz crystal microbalance setup for frequency and Q-factor measurements in gaseous and liquid environments. *Rev. Sci. Instrum.* **1995**, *66* (7), 3924−3930.
(54) Keller, C.; Kasemo, B. Surface specific kinetics of lipid vesicle adsorption measured with a quartz crystal microbalance. *Biophys. J.* **1998**, *75* (3), 1397−1402.
(55) Naumann, R.; Schiller, S. M.; Giess, F.; Grohe, B.; Hartman, K. B.; Karcher, I.; Koper, I.; Lubben, J.; Vasilev, K.; Knoll, W. Tethered lipid bilayers on ultraflat gold surfaces. *Langmuir* **2003**, *19* (13), 5435−5443.
(56) Peng, Z.; Tang, J.; Han, X.; Wang, E.; Dong, S. Formation of a supported hybrid bilayer membrane on gold: A sterically enhanced hydrophobic effect. *Langmuir* **2002**, *18* (12), 4834−4839.
(57) Höök, F.; Kasemo, B.; Nylander, T.; Fant, C.; Sott, K.; Elwing, H. Variations in coupled water, viscoelastic properties, and film thickness of a mefp-1 protein film during adsorption and cross-linking: A quartz crystal microbalance with dissipation monitoring, ellipsometry, and surface plasmon resonance study. *Anal. Chem.* **2001**, *73* (24), 5796−5804.
(58) Höök, F.; Voros, J.; Rodahl, M.; Kurrat, R.; Boni, P.; Ramsden, J. J.; Textor, M.; Spencer, N. D.; Tengvall, P.; Gold, J. A comparative study of protein adsorption on titanium oxide surfaces using in situ ellipsometry, optical waveguide lightmode spectroscopy, and quartz crystal microbalance/dissipation. *Colloids Surf., B* **2002**, *24* (2), 155−170.
(59) Jackman, J. A.; Goh, H. Z.; Zhao, Z.; Cho, N.-J. Contribution of the hydration force to vesicle adhesion on titanium oxide. *Langmuir* **2014**, *30*, 5368−5372.
(60) Bergström, L. Hamaker constants of inorganic materials. *Adv. Colloid Interface Sci.* **1997**, *70*, 125−169.
(61) Biggs, S.; Mulvaney, P. Measurement of the forces between gold surfaces in water by atomic force microscopy. *J. Chem. Phys.* **1994**, *100* (11), 8501−8505.
(62) Tristram-Nagle, S.; Petrache, H. I.; Nagle, J. F. Structure and interactions of fully hydrated dioleoylphosphatidylcholine bilayers. *Biophys. J.* **1998**, *75* (2), 917−925.
(63) Wacklin, H. P. Neutron reflection from supported lipid membranes. *Curr. Opin. Colloid Interface Sci.* **2010**, *15* (6), 445−454.
(64) Glasmästar, K.; Larsson, C.; Höök, F.; Kasemo, B. Protein adsorption on supported phospholipid bilayers. *J. Colloid Interface Sci.* **2002**, *246* (1), 40−47.
(65) Reimhult, K.; Petersson, K.; Krozer, A. QCM-D analysis of the performance of blocking agents on gold and polystyrene surfaces. *Langmuir* **2008**, *24* (16), 8695−8700.
(66) Nair, P. M.; Salaita, K.; Petit, R. S.; Groves, J. T. Using patterned supported lipid membranes to investigate the role of receptor organization in intercellular signaling. *Nat. Protoc.* **2011**, *6* (4), 523−539.

(67) Chiantia, S.; Ries, J.; Kahya, N.; Schwille, P. Combined AFM and two-focus SFCS study of raft-exhibiting model membranes. *ChemPhysChem* **2006**, *7* (11), 2409−2418.
(68) Köchy, T.; Bayerl, T. M. Lateral diffusion coefficients of phospholipids in spherical bilayers on a solid support measured by ^{2}H-nuclear-magnetic-resonance relaxation. *Phys. Rev. E* **1993**, *47* (3), 2109−2116.